Blood-based Nano-QuIC: Accelerated and Inhibitor-resistant Detection of Misfolded α-synuclein

Peter R. Christenson[1,2], Hyeonjeong Jeong[1], Manci Li[2,3], Hyerim Ahn[1], Danni Li[4], Peter A. Larsen[2,3]*, Hye Yoon Park[1]*, Sang-Hyun Oh[1,2]*

[1] Department of Electrical and Computer Engineering, University of Minnesota, Minneapolis, Minnesota 55455, United States.

[2] Minnesota Center for Prion Research and Outreach, University of Minnesota, St. Paul, Minnesota 55108, United States.

[3] Department of Veterinary and Biomedical Sciences, University of Minnesota, St. Paul, Minnesota 55108, United States.

[4] Department of Laboratory Medicine and Pathology, University of Minnesota Medical School, Minneapolis, Minnesota 55455, United States.

*Corresponding authors:

Peter A. Larsen (plarsen@umn.edu), Hye Yoon Park (hyp@umn.edu), Sang-Hyun Oh (sang@umn.edu)

Abstract

A hallmark of α-synucleinopathies including Parkinson's disease, dementia with Lewy bodies, and multiple system atrophy, is the misfolding and aggregation of α-synuclein in tissues and biological fluids. Real-time quaking-induced conversion (RT-QuIC) is a protein amplification assay providing ultrasensitive detection of disease-associated misfolded proteins yet is currently limited to invasive sample types such as cerebrospinal fluid for clinical use. More accessible sample types, especially blood, contain inhibitors that interfere with the RT-QuIC assay. Here, we show that Nanoparticle-enhanced Quaking-induced Conversion (Nano-QuIC) can greatly accelerate the detection and improves sensitivity of detection of misfolded alpha-synuclein spiked into extremely complex samples such as human plasma and whole lysed bovine blood compared to RT-QuIC. In spiked human plasma samples, Nano-QuIC showed 100-fold sensitivity improvement while doubling the speed of the reaction. In lysed whole bovine blood, Nano-QuIC detected concentrations of misfolded α-synuclein down to 90 pg/ml while RT-QuIC failed to have any detection due to the presence of strong inhibitors. Crucially, no false positives were observed in human plasma or lysed whole blood with 50 nm silica nanoparticles. This sets the groundwork for noninvasive diagnostic use of Nano-QuIC toward enabling early disease detection and management through blood-based testing.

TOC graphic

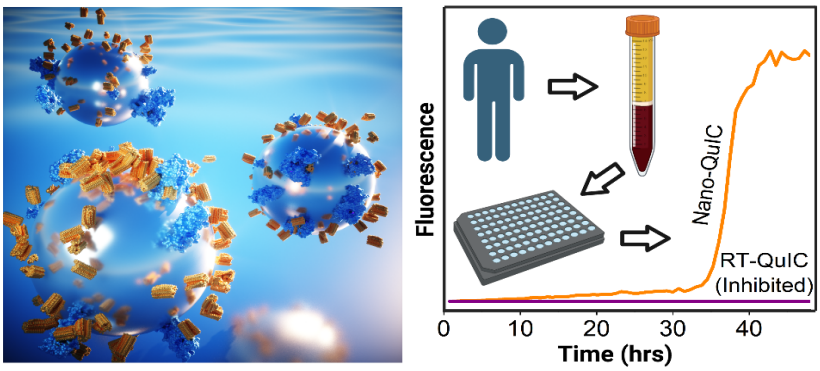

The misfolding of native α-synuclein (α-syn) protein is a hallmark of a group of neurodegenerative disorders, including Parkinson's disease (PD), dementia with Lewy bodies (DLB), and multiple system atrophy (MSA)[1–5], collectively referred to as α-synucleinopathies. In these disorders, native α-syn misfolds and aggregates into degradation-resistant amyloid deposits that are rich in β-sheet structures. The misfolded α-syn acts as a structural template, triggering other functional α-syn to misfold, thus propagating amyloid deposits, thereby causing subsequent cellular damage. While the specific roles and mechanisms of α-syn misfolding in the pathogenesis of these diseases remain elusive, there is general consensus on the potential for misfolded α-syn to be leveraged as a biomarker for diagnosis, disease progression monitoring, and therapeutic response assessment.[5–7] As such, the early and prodromal detection of misfolded α-syn for clinical applications has become a compelling area of research for α-synucleinopathies. [8–11]

Tremendous progress has been made in the quest for enhanced detection of misfolded α-syn. Currently, protein amplification assays, such as protein misfolding cyclic amplification (PMCA) and real-time quaking-induced conversion (RT-QuIC), outperform traditional immuno-based assays such as ELISA.[12] These amplification assays leverage the replicating nature of misfolded proteins. In RT-QuIC specifically, samples are incubated and shaken in solutions containing an excess of recombinant α-syn. If misfolded α-syn is present in the sample, it acts as a template seed that causes the recombinant α-syn to misfold, thus greatly increasing the number of fibrils in solution. By including amyloid-binding fluorescent dyes such as thioflavin T (ThT), the amount of misfolded α-syn in the reaction can be monitored in real time. RT-QuIC has demonstrated success for detecting misfolding proteins, including α-syn, in a wide range of neurodegenerative diseases involving protein misfolding.[13] As for α-synucleinopathies, RT-QuIC has detected the presence of pathological α-syn in several sample types including olfactory mucosa, saliva, skin, and CSF at different stages of the disease; it can even differentiate among various α-synucleinopathies using CSF.[12,14–20]

While considerable progress has been made in the clinical detection of misfolded α-syn in the CSF[7,21–23], the associated collection procedure of CSF, is a painful and invasive process that can result in bleeding into the spinal canal, extreme headaches, infections as well as a host of other symptoms. Because of these issues, CSF is not collected during routine check-ups, limiting its utility for early-stage detection of an α-synucleinopathy.

Given these challenges, the prospect of using non-invasive, readily accessible peripheral fluids such as saliva, urine, or blood[24,25], for early detection of α-synucleinopathies is highly attractive. Specifically, blood stands out as a particularly desirable target due to its frequent use in routine medical testing and the wealth of biological information it carries. Therefore, our goal in this study is to explore techniques that enable the detection of misfolded α-syn in blood samples.

Among existing assays, RT-QuIC stands as the most promising technique in this regard, but it does face significant challenges, particularly when applied to complex peripheral fluids, such as saliva, urine, and blood.[12,26] These fluids contain various components, known as inhibitors, which interfere with the seeding activity in RT-QuIC, thus hindering their direct use for the assay.[27–30] Such inhibitors have been most comprehensively documented and, at times successfully overcome, in studies of Chronic Wasting Disease (CWD).[31–35] Similarly for α-synucleinopathies, complex and costly steps, such as protein extraction from exosomes and immunoprecipitations (IP)[8,36], were needed prior to amplification using agitated incubation or RT-QuIC, to circumvent the inhibitors present in blood samples. Another impeding factor to clinical implementation is the low kinetic efficiency of these procedures, sometimes taking up to 150 hours to complete a standard test.[12]

In short, the quest to make RT-QuIC a clinically viable and translationally successful technology hinges on the ability to overcome the effects of these inhibitors in blood and other biological fluids and expediting reaction times. This focus remains imperative irrespective of the specificity among different α-syn isoforms and diseases.

Nanoparticles have been used to advance diagnostics in a number of fields.[37–42] Recently, we developed nanoparticle-enhanced quaking-induced conversion (Nano-QuIC) assay, which combines nanotechnology with traditional RT-QuIC to accelerate reaction rates, improve the sensitivity of detection, and crucially, overcome inhibitory components found in complex tissue samples.[38] Given this advancement, we sought to examine the utility of Nano-QuIC for the detection of misfolded α-syn in blood samples. Blood, owing to its non-invasive collection method and abundant biological information it provides, stands as an ideal candidate for early disease diagnostics. In this study, we delve into the effects of size and concentration of silica nanoparticles (siNPs) in the Nano-QuIC assay for blood samples. We performed tests with siNP diameters ranging from 20-100 nm with concentrations ranging from 0.1-2.5 mg/ml. We then examined the effects of pH on the α-syn-siNP interaction in RT-QuIC. Since we focus on overcoming inhibitor effects, and multiple strains and diseases create variations that complicate interpretations, we applied Nano-QuIC to detect misfolded α-syn in complex human plasma and bovine blood spiked with synthetic α-syn seeds (Fig. 1a-c). We show that Nano-QuIC can readily surmount inhibitors and detect 900 pg/ml and 90 pg/ml of spiked α-syn seeds in human plasma and whole lysed bovine blood, respectively. The significance of this lies in the high sensitivity of Nano-QuIC and its robustness to accurately detect low levels of misfolded α-syn in blood samples overcoming the limitations of conventional RT-QuIC.

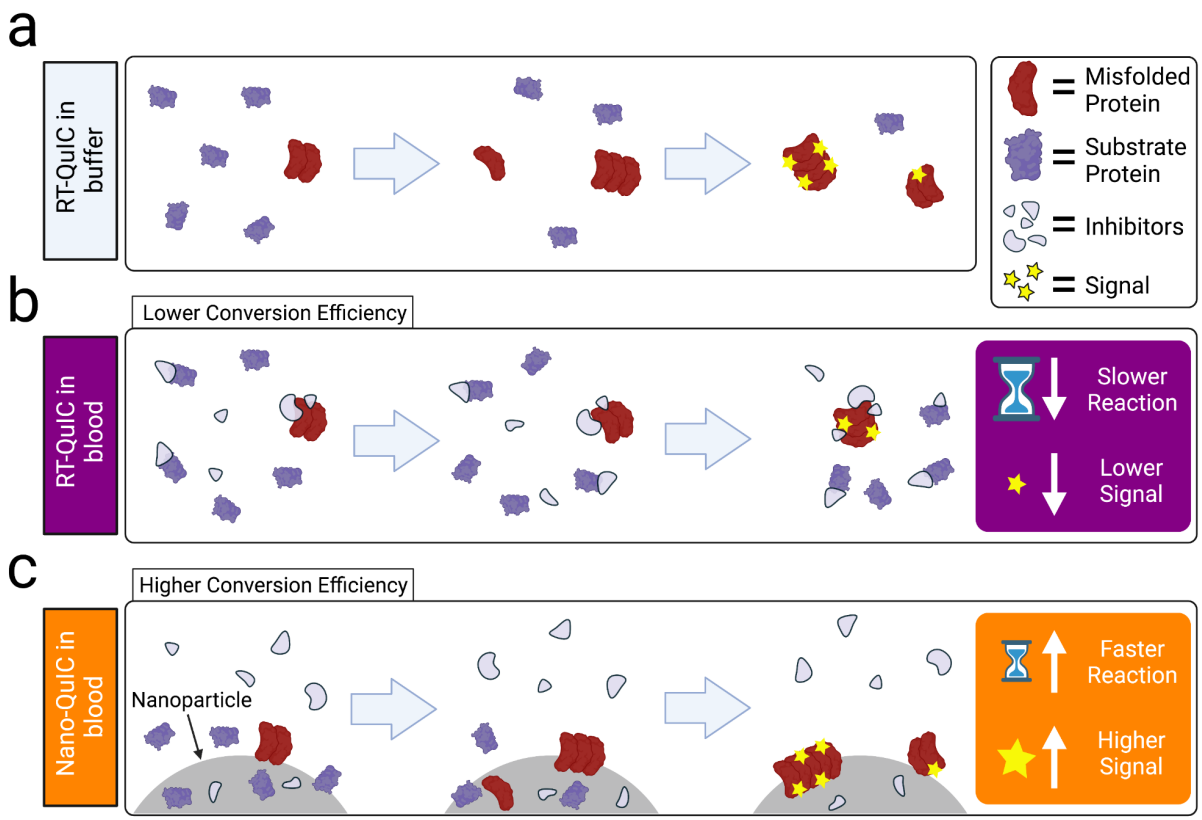

Figure 1: Overview of RT-QuIC vs. Nano-QuIC. (a) Schematic view of RT-QuIC with simple solutions. Misfolded protein catalyzes the substrate protein to misfold, triggering a chain reaction of misfolding events. (b) Possible molecular view of RT-QuIC with complex solution (e. g. whole blood or plasma) inhibiting fibril growth and detection. (c) Proposed molecular view of Nano-QuIC overcoming inhibitors in complex solution. Substrate protein adsorbs onto and/or are concentrated near the surface of the silica nanoparticle, where it is destabilized allowing for the misfolded protein to act as a template for further misfolding events.

Results

Diameter and Concentration Effects of Silica NPs (siNPs)

To examine the effect of the diameter and concentration of the siNPs, we performed siNP-QuIC across various diameters (20, 50, and 100 nm) and concentrations (0.1, 0.5, and 2.5 mg/mL) for each diameter. siNP-QuIC was held for 48 hrs at 42 °C and the rate of amyloid formation (RAF) was measured. Compared with the RAF measured without siNPs, RAF with the siNPs were all improved regardless of the diameters and concentrations (Fig. 2).

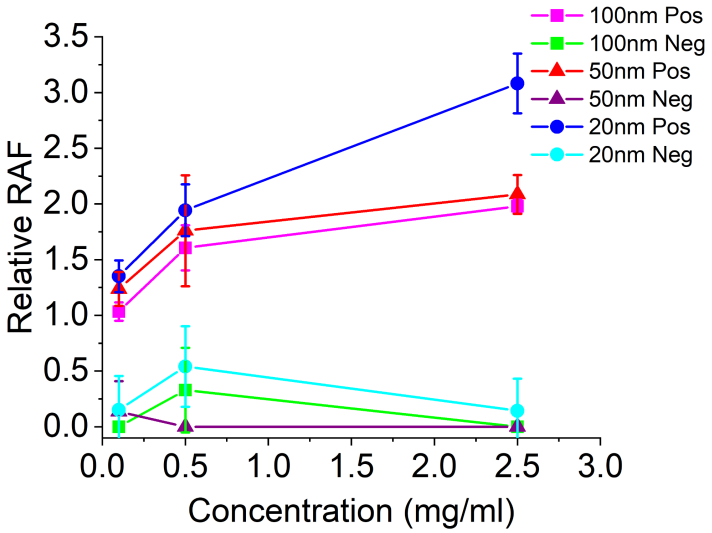

Figure 2: SiNP concentration and diameter sweeps for α-syn Nano-QuIC. Relative RAF is the ratio of the rate of amyloid formation for wells containing siNPs divided by wells without AuNPs.

As the diameter of siNPs became smaller, the RAF value became larger. However, in the RAF of 20 nm siNPs', false seeding was observed in some of the negative controls, which would lead to lower accuracy of α-syn detection. On the other hand, in the same diameter of siNPs, as concentration increases, the RAF also improved (Fig. 2). As a result, 50 nm siNPs, with 2.5 mg/mL was deemed best because it gave significant improvement to the RAF while showing no false seeding.

Investigating pH Effects

To determine the effects of pH on Nano-QuIC, we performed Nano-QuIC across a pH range (6.3, 6.7, 7.1, and 7.5) for 50 nm siNPs at a concentration of 2.5 mg/ml. This pH range was selected within the buffering capacity of phosphate buffers. We then measured the RAFs and found that as the pH of the master mix became lower, the RAF values were increased (Fig. 3), with the fastest detection time (9.5 hrs) measured at pH 6.3. Notably, in the negative control wells that were not seeded with misfolded α-syn, no seeding activity was detected before the 42

hr mark. As a result, pH 6.3 for the master mix was considered optimal for detecting misfolded α-syn.

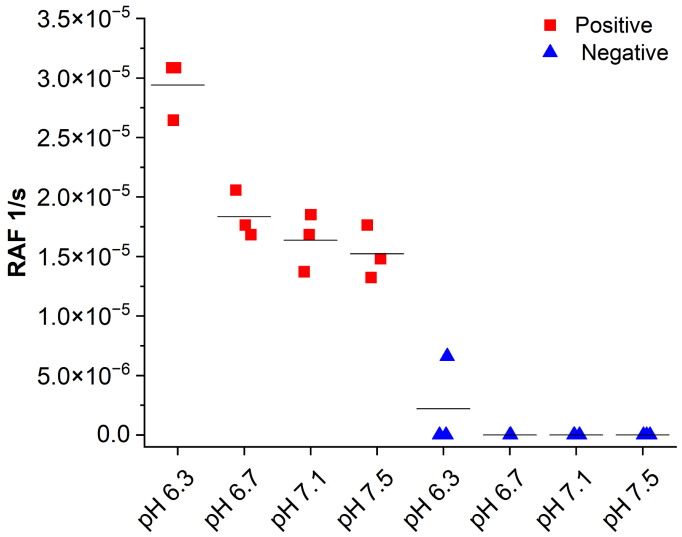

Figure 3: Effects of pH on the RAF of α-syn Nano-QuIC reactions. The speed of the reaction increases as the pH drops.

Detection of misfolded a-syn in human plasma

In previous work, we showed that Nano-QuIC greatly reduces the effect of inhibitors in the lymph tissue of wild white-tailed deer infected with CWD.[38] In this study, we extended our focus to human plasma samples. To create misfolded α-syn spikes, RT-QuIC reactions with concentrations of 0.09 mg/ml α-syn were shaken till spontaneous aggregation occurred. These spontaneous seeds were then aliquoted and stored for future use.

Misfolded α-syn spikes at an in plasma concentration of 9 µg/ml were serially diluted 10-fold in human plasma down to 90 pg/ml. Each of the 10-fold dilution series was diluted 100-fold in SDS PBS and added to both RT-QuIC and Nano-QuIC reactions. No other extractions or sample preparation steps were performed. We found that Nano-QuIC could detect the misfolded α-syn down 900 pg/ml, whereas RT-QuIC only detected seeding down to 90 ng/ml (Fig. 4a). Importantly, there was no false seeding shown in the negative control. Additionally, for all wells

showing seeding activity, Nano-QuIC detection time was on average 2X faster than RT-QuIC of the same spike dilution (Fig. 4 a&b). Although ~20 hours average detection time for Nano-QuIC still seem lengthy, this represents a significant gain in throughput since the average reaction time is cut by half from ~40 hours (for RT-QuIC) to 20 hours (for Nano-QuIC).

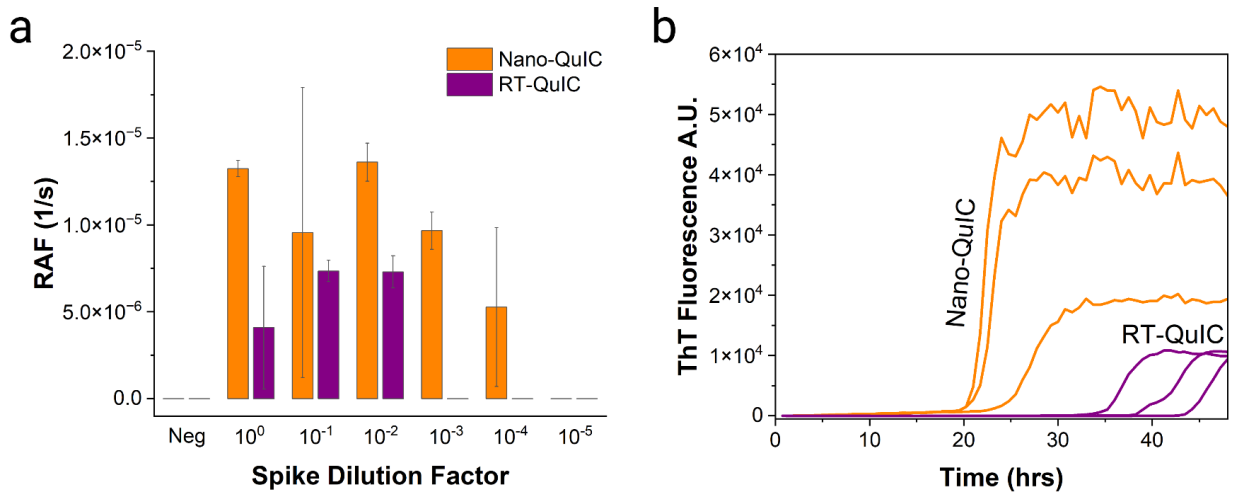

Figure 4: (a) Dilution of misfolded α-syn spike in human plasma from 9 µg/ml to 90 pg/ml. Nano-QuIC overcomes inhibitors to allow a 100-fold improvement in sensitivity. (b) ThT fluorescence curves for human plasma samples spiked to 90ng/ml (dilution 10^{-3}) misfolded α-syn.

Detection of misfolded α-syn in bovine whole blood

Our experiments using human plasma showed proof-of-concept results for using Nano-QuIC to overcome blood-borne inhibitors to detect misfolded α-syn even in complex biological samples. Historically, blood has been a challenging sample type for QuIC-like reactions due to the presence of various inhibitors.[27,43,44] To further validate the robustness of Nano-QuIC and its ability to negate these inhibitory effects, we expanded our testing scope to include misfolded α-syn spike into lysed whole bovine blood. We utilized bovine whole blood for two reasons. First it presents an even higher level of complexity than human plasma, showcasing the ability of

Nano-QuIC to function effectively in extremely challenging biological matrices. Second, the ease of acquiring a large volume of bovine blood allowed us to run a series of Nano-QuIC experiments to develop optimal protocols.

Misfolded α-syn was spiked into bovine blood to a concentration of 9 µg/ml. This sample was then serially diluted 10-fold in bovine blood down to 90 pg/ml. Each of the 10-fold dilution series was further diluted 100-fold in SDS PBS and added to both RT-QuIC and Nano-QuIC reactions. No other extractions or sample preparation steps were performed. Our results demonstrate that Nano-QuIC was able to detect the misfolded α-syn down to a concentration of 90 pg/ml. In stark contrast, RT-QuIC failed to detect any presence of misfolded α-syn due to the presence of inhibitors (Fig. 5 a-b). Importantly, our negative control showed no seeding, underscoring the specificity of our Nano-QuIC assay.

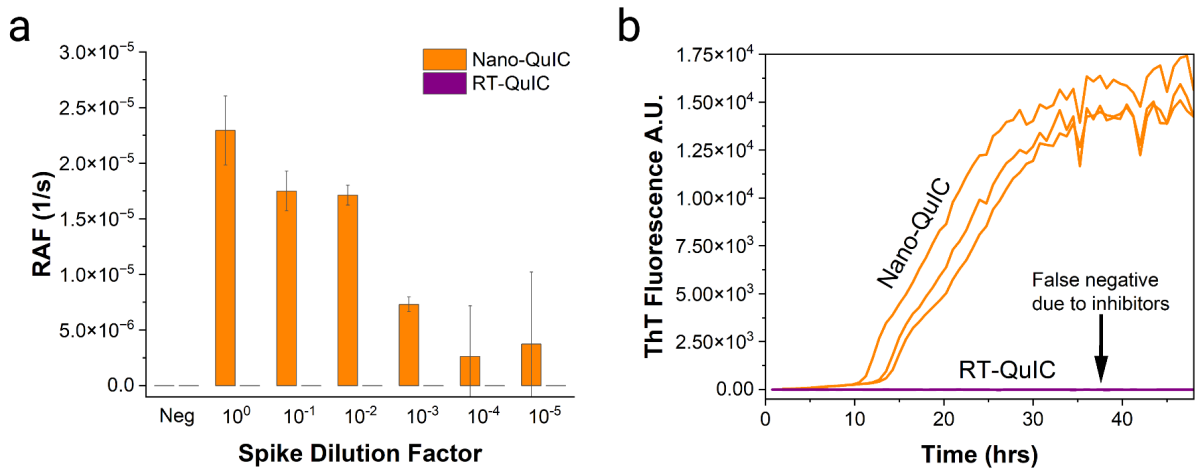

Figure 5: (a) Dilution of misfolded α-syn spike in bovine whole blood from 9 µg/ml to 90 pg/ml. While conventional RT-QuIC shows no detection, Nano-QuIC shows detection down to 90 pg/ml (b) ThT fluorescence curves for bovine blood samples spiked to 9 µg/ml (dilution 10^0) misfolded α-syn.

Discussion

Our study shows the enhanced efficiency of Nano-QuIC reactions utilizing 50 nm siNPs, which significantly expedited the rate of amyloid formation (cutting times to detection in half) while displaying no false seeding. By sweeping the pH of our Nano-QuIC reactions, we showed that seeding activity is more efficiently detected at lower pH, supporting the hypothesis that electrostatic charge plays a role in the mechanism of Nano-QuIC. We successfully leveraged Nano-QuIC to detect misfolded α-syn as low as 900 pg/ml in human blood plasma (Fig. 4) and 90 pg/ml in lysed whole bovine blood (Fig. 5), demonstrating the potential use of Nano-QuIC for detection of disease associated α-syn in blood.

Human plasma, often used in routine diagnostic assays due to its noninvasive acquisition process, represents an ideal target for assay development. Whole bovine blood was used because it serves as an excellent model displaying the complexity of real biological samples. Lysed blood maximizes inhibitors thus representing an extremely challenging sample. The abundance of bovine blood also facilitates the early stages of our protocol development.

We observed the 50 nm siNPs in reactions at pH 6.3 gave the fastest kinetics while maintaining minimal false seeding (Figs. 2 and 3). Previously, we reasoned that the siNPs accelerated the reaction kinetics of misfolded protein aggregation because substrate proteins adsorbed onto the silica surface partly through electrostatic interactions.[38] The adsorbed protein is more concentrated at the surface and likely changes conformation to a state more readily misfolded[45–47] (Fig. 1). Above the isoelectric point of α-syn (~4.7), the net charge of α-syn is negative, which likely decreases the amount of α-syn interacting with the negatively charged siNPs. As the pH decreases, the net charge on the α-syn becomes closer to neutral charge thus allowing it to interact more efficiently with the negatively charged siNP possibly through hydrophobic, hydrophilic, and local electrostatic interactions.[42,48] This trend, reflected in Fig. 3, shows that as the pH of the solution decreases the interactions of the α-syn with the siNPs

increases as seen by the rate of amyloid formation increasing. Additionally, it has been reported that α-syn can interact with negatively charged gold nanoparticles at pH around 6.2. [49]

We have demonstrated that Nano-QuIC is a promising technique to overcome inhibitory barriers commonly associated with blood/plasma samples in conventional RT-QuIC assays. Whole blood samples are extremely complex and challenging to diagnostics. In samples such as CSF, blood contamination is thought to greatly interfere with QuIC diagnostics.[27,44] Even in the presence robust inhibitors present in whole blood, Nano-QuIC successfully detected misfolded α-syn down to 90 pg/ml, whereas RT-QuIC failed to detect any presence at any dilutions (Fig. 5 a-b). With human plasma, Nano-QuIC again outperformed RT-QuIC, having no false positive replicates while detecting misfolded α-syn at a level 900 pg/ml, a 100-fold lower than RT-QuIC (Fig. 4 a-b).

In conclusion, the unique ability of Nano-QuIC to overcome inhibitors, enhance diagnostic sensitivity and specificity, and accelerate detection time, collectively mark a significant advance over traditional RT-QuIC diagnostics. These improvements are especially useful for blood samples, which have historically been plagued by inhibitors that render them unsuitable for clinical applications of RT-QuIC. The promising results from our proof-of-concept experiments set the foundation for subsequent research. Future work should focus on testing Nano-QuIC using blood samples from patients living with α-synucleinopathies such Parkinson's disease, dementia with Lewy bodies, and multiple system atrophy. Should Nano-QuIC become integrated into clinical diagnostics, it could not only facilitate early disease detection but also aid in patient prognoses, and assess drug efficacy, potentially impacting the way we could manage these debilitating conditions.

Author Contributions. S.H.O. conceived the study. P.R.C., H.J, H.A. and M.L. performed molecular experiments. P.R.C., M.L., H.J, H.A., S.H.O., H.Y.P. and P.A.L. assisted with experimental design and interpreted the results. D.L. provided human blood plasma samples. P.R.C. and M.L. performed statistical analyses. S.H.O., H.Y.P. and P.A.L. oversaw the research. All authors wrote and contributed to the final manuscript.

Funding Sources

P.R.C. was supported by the Mistletoe Research Fellowship from the Momental Foundation and the Interdisciplinary Doctoral Fellowship from the U. of Minnesota. H.J., H.A., H.Y.P. acknowledge the startup fund to H.Y.P from the University of Minnesota. S.-H.O. acknowledges support from the Sanford P. Bordeau Chair at the University of Minnesota and the McKnight Foundation. P.A.L. and M.L. acknowledge startup funds through the Minnesota Agricultural, Research, Education, Extension and Technology Transfer (AGREETT) program.

Notes

P.R.C., P.A.L. and S.-H.O. declare the following competing financial interest: A provisional patent has been filed, which covers specific ideas, design, and protocols outlined within this paper. All other authors declare no competing interests.

Acknowledgments. The authors thank NIH Rocky Mountain Labs, especially Byron Caughey, Andrew Hughson, and Christina Orrù for training and assistance with the implementation of RT-QuIC. Luciano Caixeta provided cow blood samples. Gage Rowden provided valuable assistance. S. Stone provided valuable logistical assistance with our molecular work.

References

(1) Lashuel, H. A.; Overk, C. R.; Oueslati, A.; Masliah, E. The Many Faces of α-Synuclein: From Structure and Toxicity to Therapeutic Target. *Nat. Rev. Neurosci.* **2013**, *14*, 38–48.

(2) Spillantini, M. G.; Schmidt, M. L.; Lee, V. M.; Trojanowski, J. Q.; Jakes, R.; Goedert, M. Alpha-Synuclein in Lewy Bodies. *Nature* **1997**, *388* (6645), 839–840.

(3) Gai, W. P.; Power, J. H. T.; Blumbergs, P. C.; Blessing, W. W. Multiple-System Atrophy: A New α-Synuclein Disease? *Lancet* **1998**, *352* (9127), 547–548.

(4) Ebrahimi-Fakhari, D.; Wahlster, L.; McLean, P. J. Protein Degradation Pathways in Parkinson's Disease: Curse or Blessing. *Acta Neuropathol.* **2012**, *124* (2), 153–172.

(5) Srivastava, A.; Alam, P.; Caughey, B. RT-QuIC and Related Assays for Detecting and Quantifying Prion-like Pathological Seeds of α-Synuclein. *Biomolecules* **2022**, *12* (4), 576.

(6) Parnetti, L.; Gaetani, L.; Eusebi, P.; Paciotti, S.; Hansson, O.; El-Agnaf, O.; Mollenhauer, B.; Blennow, K.; Calabresi, P. CSF and Blood Biomarkers for Parkinson's Disease. *Lancet Neurol.* **2019**, *18* (6), 573–586.

(7) Siderowf, A.; Concha-Marambio, L.; Lafontant, D.-E.; Farris, C. M.; Ma, Y.; Urenia, P. A.; Nguyen, H.; Alcalay, R. N.; Chahine, L. M.; Foroud, T.; Galasko, D.; Kieburtz, K.; Merchant, K.; Mollenhauer, B.; Poston, K. L.; Seibyl, J.; Simuni, T.; Tanner, C. M.; Weintraub, D.; Videnovic, A.; Choi, S. H.; Kurth, R.; Caspell-Garcia, C.; Coffey, C. S.; Frasier, M.; Oliveira, L. M. A.; Hutten, S. J.; Sherer, T.; Marek, K.; Soto, C.; Parkinson's Progression Markers Initiative. Assessment of Heterogeneity among Participants in the Parkinson's Progression Markers Initiative Cohort Using α-Synuclein Seed Amplification: A Cross-Sectional Study. *Lancet Neurol.* **2023**, *22* (5), 407–417.

(8) Okuzumi, A.; Hatano, T.; Matsumoto, G.; Nojiri, S.; Ueno, S.-I.; Imamichi-Tatano, Y.; Kimura, H.; Kakuta, S.; Kondo, A.; Fukuhara, T.; Li, Y.; Funayama, M.; Saiki, S.; Taniguchi, D.; Tsunemi, T.; McIntyre, D.; Gérardy, J.-J.; Mittelbronn, M.; Kruger, R.; Uchiyama, Y.; Nukina, N.; Hattori, N. Propagative α-Synuclein Seeds as Serum Biomarkers for Synucleinopathies. *Nat. Med.* **2023**, *29*, 1448–1455.

(9) Delenclos, M.; Jones, D. R.; McLean, P. J.; Uitti, R. J. Biomarkers in Parkinson's Disease: Advances and Strategies. *Parkinsonism Relat. Disord.* **2016**, *22*, S106–S110.

(10) Singer, W.; Schmeichel, A. M.; Shahnawaz, M.; Schmelzer, J. D.; Sletten, D. M.; Gehrking, T. L.; Gehrking, J. A.; Olson, A. D.; Suarez, M. D.; Misra, P. P.; Soto, C.; Low, P. A. Alpha-Synuclein Oligomers and Neurofilament Light Chain Predict Phenoconversion of Pure Autonomic Failure. *Ann. Neurol.* **2021**, *89* (6), 1212–1220.

(11) Singer, W.; Schmeichel, A. M.; Shahnawaz, M.; Schmelzer, J. D.; Boeve, B. F.; Sletten, D. M.; Gehrking, T. L.; Gehrking, J. A.; Olson, A. D.; Savica, R.; Suarez, M. D.; Soto, C.; Low, P. A. Alpha-Synuclein Oligomers and Neurofilament Light Chain in Spinal Fluid Differentiate Multiple System Atrophy from Lewy Body Synucleinopathies. *Ann. Neurol.* **2020**, *88* (3), 503–512.

(12) Concha-Marambio, L.; Pritzkow, S.; Shahnawaz, M.; Farris, C. M.; Soto, C. Seed Amplification Assay for the Detection of Pathologic Alpha-Synuclein Aggregates in Cerebrospinal Fluid. *Nat. Protoc.* **2023**, *18* (4), 1179–1196.

(13) Candelise, N.; Baiardi, S.; Franceschini, A.; Rossi, M.; Parchi, P. Towards an Improved Early Diagnosis of Neurodegenerative Diseases: The Emerging Role of in Vitro Conversion Assays for Protein Amyloids. *Acta Neuropathol Commun* **2020**, *8* (1), 117.

(14) Coughlin, D. G.; Irwin, D. J. Fluid and Biopsy Based Biomarkers in Parkinson's Disease. *Neurotherapeutics* **2023**. https://doi.org/10.1007/s13311-023-01379-z.

(15) Bongianni, M.; Catalan, M.; Perra, D.; Fontana, E.; Janes, F.; Bertolotti, C.; Sacchetto, L.; Capaldi, S.; Tagliapietra, M.; Polverino, P.; Tommasini, V.; Bellavita, G.; Kachoie, E. A.; Baruca, R.; Bernardini, A.; Valente, M.; Fiorini, M.; Bronzato, E.; Tamburin, S.; Bertolasi, L.; Brozzetti, L.; Cecchini, M. P.; Gigli, G.; Monaco, S.; Manganotti, P.; Zanusso, G. Olfactory Swab Sampling Optimization for α-Synuclein Aggregate Detection in Patients with Parkinson's Disease. *Transl. Neurodegener.* **2022**, *11* (1), 37.

(16) Abd-Elhadi, S.; Basora, M.; Vilas, D.; Tolosa, E.; Sharon, R. Total α-Synuclein Levels in Human Blood Cells, CSF, and Saliva Determined by a Lipid-ELISA. *Anal. Bioanal. Chem.* **2016**, *408* (27), 7669–7677.

(17) Manne, S.; Kondru, N.; Hepker, M.; Jin, H.; Anantharam, V.; Lewis, M.; Huang, X.; Kanthasamy, A.; Kanthasamy, A. G. Ultrasensitive Detection of Aggregated α-Synuclein in Glial Cells, Human Cerebrospinal Fluid, and Brain Tissue Using the RT-QuIC Assay: New High-Throughput Neuroimmune Biomarker Assay for Parkinsonian Disorders. *J. Neuroimmune Pharmacol.* **2019**, *14* (3), 423–435.

(18) Manne, S.; Kondru, N.; Jin, H.; Serrano, G. E.; Anantharam, V.; Kanthasamy, A.; Adler, C. H.; Beach, T. G.; Kanthasamy, A. G. Blinded RT-QuIC Analysis of α-Synuclein Biomarker in Skin Tissue From Parkinson's Disease Patients. *Mov. Disord.* **2020**, *35* (12), 2230–2239.

(19) De Luca, C. M. G.; Elia, A. E.; Portaleone, S. M.; Cazzaniga, F. A.; Rossi, M.; Bistaffa, E.; De Cecco, E.; Narkiewicz, J.; Salzano, G.; Carletta, O.; Romito, L.; Devigili, G.; Soliveri, P.; Tiraboschi, P.; Legname, G.; Tagliavini, F.; Eleopra, R.; Giaccone, G.; Moda, F. Efficient RT-QuIC Seeding Activity for α-Synuclein in Olfactory Mucosa Samples of Patients with Parkinson's Disease and Multiple System Atrophy. *Transl. Neurodegener.* **2019**, *8*, 24.

(20) Shahnawaz, M.; Mukherjee, A.; Pritzkow, S.; Mendez, N.; Rabadia, P.; Liu, X.; Hu, B.; Schmeichel, A.; Singer, W.; Wu, G.; Tsai, A.-L.; Shirani, H.; Nilsson, K. P. R.; Low, P. A.; Soto, C. Discriminating α-Synuclein Strains in Parkinson's Disease and Multiple System Atrophy. *Nature* **2020**, *578* (7794), 273–277.

(21) Groveman, B. R.; Orrù, C. D.; Hughson, A. G.; Raymond, L. D.; Zanusso, G.; Ghetti, B.; Campbell, K. J.; Safar, J.; Galasko, D.; Caughey, B. Rapid and Ultra-Sensitive Quantitation of Disease-Associated α-Synuclein Seeds in Brain and Cerebrospinal Fluid by αSyn RT-QuIC. *Acta Neuropathol Commun* **2018**, *6* (1), 7.

(22) Fairfoul, G.; McGuire, L. I.; Pal, S.; Ironside, J. W.; Neumann, J.; Christie, S.; Joachim, C.; Esiri, M.; Evetts, S. G.; Rolinski, M.; Baig, F.; Ruffmann, C.; Wade-Martins, R.; Hu, M. T. M.; Parkkinen, L.; Green, A. J. E. Alpha-Synuclein RT-QuIC in the CSF of Patients with Alpha-Synucleinopathies. *Ann Clin Transl Neurol* **2016**, *3* (10), 812–818.

(23) Danzer, K. M.; Kranich, L. R.; Ruf, W. P.; Cagsal-Getkin, O.; Winslow, A. R.; Zhu, L.; Vanderburg, C. R.; McLean, P. J. Exosomal Cell-to-Cell Transmission of Alpha Synuclein Oligomers. *Mol. Neurodegener.* **2012**, *7*, 42.

(24) Nakai, M.; Fujita, M.; Waragai, M.; Sugama, S.; Wei, J.; Akatsu, H.; Ohtaka-Maruyama, C.; Okado, H.; Hashimoto, M. Expression of Alpha-Synuclein, a Presynaptic Protein Implicated in Parkinson's Disease, in Erythropoietic Lineage. *Biochem. Biophys. Res. Commun.* **2007**, *358* (1), 104–110.

(25) Abd Elhadi, S.; Grigoletto, J.; Poli, M.; Arosio, P.; Arkadir, D.; Sharon, R. α-Synuclein in Blood Cells Differentiates Parkinson's Disease from Healthy Controls. *Ann Clin Transl Neurol* **2019**, *6* (12), 2426–2436.

(26) Masson, J.-F. Surface Plasmon Resonance Clinical Biosensors for Medical Diagnostics. *ACS Sens* **2017**, *2* (1), 16–30.

(27) Cramm, M.; Schmitz, M.; Karch, A.; Mitrova, E.; Kuhn, F.; Schroeder, B.; Raeber, A.; Varges, D.; Kim, Y.-S.; Satoh, K.; Collins, S.; Zerr, I. Stability and Reproducibility Underscore Utility of RT-QuIC for Diagnosis of Creutzfeldt-Jakob Disease. *Mol. Neurobiol.* **2016**, *53* (3), 1896–1904.

(28) Kuzkina, A.; Bargar, C.; Schmitt, D.; Rößle, J.; Wang, W.; Schubert, A.-L.; Tatsuoka, C.; Gunzler, S. A.; Zou, W.-Q.; Volkmann, J.; Sommer, C.; Doppler, K.; Chen, S. G. Diagnostic Value of Skin RT-QuIC in Parkinson's Disease: A Two-Laboratory Study. *NPJ Parkinsons Dis* **2021**, *7* (1), 99.

(29) Bargar, C.; Wang, W.; Gunzler, S. A.; LeFevre, A.; Wang, Z.; Lerner, A. J.; Singh, N.; Tatsuoka, C.; Appleby, B.; Zhu, X.; Xu, R.; Haroutunian, V.; Zou, W.-Q.; Ma, J.; Chen, S. G. Streamlined Alpha-Synuclein RT-QuIC Assay for Various Biospecimens in Parkinson's Disease and Dementia with Lewy Bodies. *Acta Neuropathol Commun* **2021**, *9* (1), 62.

(30) Altug, H.; Oh, S.-H.; Maier, S. A.; Homola, J. Advances and Applications of Nanophotonic Biosensors. *Nat. Nanotechnol.* **2022**, *17* (1), 5–16.

(31) Henderson, D. M.; Davenport, K. A.; Haley, N. J.; Denkers, N. D.; Mathiason, C. K.; Hoover, E. A. Quantitative Assessment of Prion Infectivity in Tissues and Body Fluids by Real-Time Quaking-Induced Conversion. *J. Gen. Virol.* **2015**, *96* (Pt 1), 210–219.

(32) C. E. Hoover, K. A. Davenport, D. M. Henderson, M. D. Zabel, E. A. Hoover Endogenous Brain Lipids Inhibit Prion Amyloid Formation In Vitro. *J. Virol.* **2017**, *91*, 1–12.

(33) Davenport, K. A.; Hoover, C. E.; Denkers, N. D.; Mathiason, C. K.; Hoover, E. A. Modified Protein Misfolding Cyclic Amplification Overcomes Real-Time Quaking-Induced Conversion Assay Inhibitors in Deer Saliva To Detect Chronic Wasting Disease Prions. *J. Clin. Microbiol.* **2018**, *56* (9). https://doi.org/10.1128/JCM.00947-18.

(34) Li, M.; Schwabenlander, M. D.; Rowden, G. R.; Schefers, J. M.; Jennelle, C. S.; Carstensen, M.; Seelig, D.; Larsen, P. A. RT-QuIC Detection of CWD Prion Seeding Activity in White-Tailed Deer Muscle Tissues. *Sci. Rep.* **2021**, *11* (1), 16759.

(35) Bistaffa, E.; Vuong, T. T.; Cazzaniga, F. A.; Tran, L.; Salzano, G.; Legname, G.; Giaccone, G.; Benestad, S. L.; Moda, F. Use of Different RT-QuIC Substrates for Detecting CWD Prions in the Brain of Norwegian Cervids. *Sci. Rep.* **2019**, *9* (1), 18595.

(36) Kluge, A.; Bunk, J.; Schaeffer, E.; Drobny, A.; Xiang, W.; Knacke, H.; Bub, S.; Lückstädt, W.; Arnold, P.; Lucius, R.; Berg, D.; Zunke, F. Detection of Neuron-Derived Pathological α-Synuclein in Blood. *Brain* **2022**, *145* (9), 3058–3071.

(37) Kumar, A.; Kim, S.; Nam, J.-M. Plasmonically Engineered Nanoprobes for Biomedical Applications. *J. Am. Chem. Soc.* **2016**, *138* (44), 14509–14525.

(38) Christenson, P. R.; Li, M.; Rowden, G.; Larsen, P. A.; Oh, S.-H. Nanoparticle-Enhanced RT-QuIC (Nano-QuIC) Diagnostic Assay for Misfolded Proteins. *Nano Lett.* **2023**, *23* (9), 4074–4081.

(39) Belushkin, A.; Yesilkoy, F.; Altug, H. Nanoparticle-Enhanced Plasmonic Biosensor for Digital Biomarker Detection in a Microarray. *ACS Nano* **2018**, *12* (5), 4453–4461.

(40) Akkilic, N.; Geschwindner, S.; Höök, F. Single-Molecule Biosensors: Recent Advances and Applications. *Biosens. Bioelectron.* **2020**, *151*, 111944.

(41) Jackman, J. A.; Rahim Ferhan, A.; Cho, N.-J. Nanoplasmonic Sensors for Biointerfacial Science. *Chem. Soc. Rev.* **2017**, *46* (12), 3615–3660.

(42) Christenson, P. R.; Li, M.; Rowden, G.; Schwabenlander, M. D.; Wolf, T. M.; Oh, S.-H.; Larsen, P. A. A Field-Deployable Diagnostic Assay for the Visual Detection of Misfolded Prions. *Sci. Rep.* **2022**, *12* (1), 12246.

(43) Coysh, T.; Mead, S. The Future of Seed Amplification Assays and Clinical Trials. *Front. Aging Neurosci.* **2022**, *14*, 872629.

(44) Dong, T.-T.-T.; Satoh, K. The Latest Research on RT-QuIC Assays-A Literature Review. *Pathogens* **2021**, *10* (3), 305.

(45) Grigolato, F.; Arosio, P. The Role of Surfaces on Amyloid Formation. *Biophys. Chem.* **2021**, *270*, 106533.

(46) Zhang, D.; Neumann, O.; Wang, H.; Yuwono, V. M.; Barhoumi, A.; Perham, M.; Hartgerink, J. D.; Wittung-Stafshede, P.; Halas, N. J. Gold Nanoparticles Can Induce the Formation of Protein-Based Aggregates at Physiological pH. *Nano Lett.* **2009**, *9* (2), 666–671.

(47) John, T.; Gladytz, A.; Kubeil, C.; Martin, L. L.; Risselada, H. J.; Abel, B. Impact of Nanoparticles on Amyloid Peptide and Protein Aggregation: A Review with a Focus on Gold Nanoparticles. *Nanoscale* **2018**, *10* (45), 20894–20913.

(48) Kim, Y.; Park, J.-H.; Lee, H.; Nam, J.-M. How Do the Size, Charge and Shape of Nanoparticles Affect Amyloid β Aggregation on Brain Lipid Bilayer? *Sci. Rep.* **2016**, *6*, 19548.

(49) Alvarez, Y. D.; Fauerbach, J. A.; Pellegrotti, J. V.; Jovin, T. M.; Jares-Erijman, E. A.; Stefani, F. D. Influence of Gold Nanoparticles on the Kinetics of α-Synuclein Aggregation. *Nano Lett.* **2013**, *13* (12), 6156–6163.